Hardware Verification of an Ultra-miniature Computational Diffractive Imager

Patrick R. Gill and David G. Stork
Rambus Labs
1050 Enterprise Way, Suite 700
Sunnyvale, CA 94089 USA
{*pgill,dstork*}*@rambus.com*

Abstract: We describe the first hardware implementation of a new class of ultra-miniature lensless diffraction-based computational imager.

OCIS codes: 110.0110, 050.1970, 100.1390, 110.1758, 130.3120, 130.6010

1. Computational diffractive imaging

Ever since Dowski and Cathey's pioneering work on cubic phase plates, [1] computational optical imaging has relied almost exclusively upon reflective or refractive optics paired with computation—sometimes jointly designed [2]—to enhance imaging performance and functionality. In this paradigm, images are computed (not captured) as much of the digital image production burden is shifted from the optics to the signal processing, thereby providing greater freedom in the design of the optics. Gill et al. introduced *diffractive* computational imaging based on the Talbot effect and prototyped an integrated CMOS image sensor—the Planar Fourier Capture Array—that contained two planes of metal lines that acted as amplitude diffraction gratings. [3] Their imager possessed a number of technical problems that limited its use in commercial applications, however: the sensor response was sensitive to variability in the separation of the manufactured gratings and to changes in the incident wavelength, the sensor was difficult to calibrate, its light sensitivity was low, and others. Our prior work addressed those limitations through mathematical analyses and simulations and led to designs for a new class of diffractive imager employing special spiral phase anti-symmetric binary gratings. [4–7] Here we report the first hardware verification of our theory and imager functionality.

2. Hardware construction

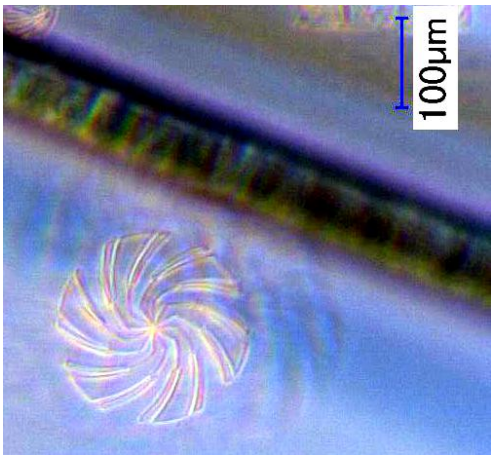

Fig. 1. Optical micrograph of our spiral binary anti-symmetric phase grating, 212 μm across, with a human hair for size comparison. The raw photodetector signals are captured by an array of pixels on the integrated CMOS image sensor beneath (not shown). Light passes through the grating from a field of view subtending 100° and strikes a photodetector sensor area of 400 × 400 pixels.

Our experimental platform consists of a 4 × 5.5 *mm* silicate binary phase grating plate bearing 29 optical gratings of various spiral, linear, and special-purpose shapes, designed to serve a range of imaging and computer vision applications. The overall grating thickness is 500 μm with ridges of height 1.5 μm, which corresponds to the required phase delay of $\lambda/2$ for 600 *nm* light ($\Delta n \simeq 0.2$). [8] The plate is mounted on an Aptina MT9J003 10 *MP* sensor [9] connected through a USB 3.0 port to a PC for sensor control and signal readout. The 12-bit pixels with 1.67 μm pitch are and polychromatic (no color filter array). There is no limitation, in principle, to the sampling rate of such a sensor architecture, but our prototype can be sampled at rates up to 27 *Hz*—a limitation imposed by this Aptina sensor interface. We used a digital projector a distance of 15 *cm* from the sensor for presentation of calibration patterns and targets. Our spiral gratings for imaging applications act as a two-dimensional "chirp" and preserve the full Fourier image information as captured on the underlying photodetector

array. We report here results from just one grating—a binary anti-symmetric spiral phase grating 212 μm in diameter designed for imaging applications (Fig. 1). We verified experimentally that indeed our grating preserved the two-dimensional Fourier spectrum (up to the two-dimensional Nyquist rate) and—most importantly—that there are no zeros in this spectrum.

3. Image computation algorithms

As described in greater detail elsewhere, [6, 7] we denote the input image as a vector $\mathbf{x}$, the raw signals on the sensor signals as $\mathbf{y}$, and the real grating transfer matrix as $\mathbf{A}$, all real, non-negative valued. The linear imaging model is then $\mathbf{y} = \mathbf{A}\mathbf{x} + \mathbf{n}$, where $\mathbf{n}$ is pixel-wise random noise in the sensor and circuitry. There are two signal processing tasks: 1) Calibrating the optics, i.e., estimating $\mathbf{A}$ for the as-built system, and 2) Computing the image from the estimated $\mathbf{A}$ and the raw sensor signals, $\mathbf{y}$. All such computations were done in *Matlab* on a PC.

3.1. Optics calibration

The calibration task is to estimate $\mathbf{A}$ for the grating optics, as built, given a matrix of designed calibration target patterns. While Hadamard patterns have desirable orthogonality properties, their -1 entries cannot be directly presented by physical light. We therefore presented two non-negative complementary patterns for each Hadamard pattern and subtracted their associated sensor signals to get $\mathbf{Y}$. (We used $m = 16384$ Hadamard patterns, each of size 128×128.) In the linear model (i.e., $\mathbf{Y} = \mathbf{A}\mathbf{X} + \mathbf{N}$), the transfer matrix $\mathbf{A}$ can be estimated noting $\mathbf{Y}\mathbf{X}^t = \mathbf{A}\mathbf{X}\mathbf{X}^t + \mathbf{N}\mathbf{X}^t$ and (due to the orthogonality of the Hadamard patterns) $\mathbf{X}\mathbf{X}^t = m\mathbf{I}$. The estimate is then $\hat{\mathbf{A}} = \mathbf{Y}\mathbf{X}^t/m$ with $\mathbf{A} - \hat{\mathbf{A}} \simeq \mathbf{N}\mathbf{X}^t/m$. This calibration method reduces significantly the effects of noise in sensor pixels when there is low incident light and is noise-optimal under a constrained maximum display intensity. The larger the number of such calibration patterns m, the more accurate is the estimate of $\mathbf{A}$ and thus the higher the fidelity of the computed images. Such calibration is performed once, offline, for each sensor design. [10]

The scalar *condition number* of our transfer matrix, $\kappa(\mathbf{A})$, is the ratio of the magnitude of its largest eigenvalue to its smallest, $|\lambda_{max}/\lambda_{min}|$, and yields a rough estimate of how accurately the inverse of $\mathbf{A}$ can be computed (Sect. 3.2). In our application, $\kappa(\mathbf{A})$ thus also governs the theoretical accuracy of estimation of the scene, $\mathbf{x}$. A low condition number—e.g., the lowest possible, $\kappa(\mathbf{I}) = 1$ for an identity matrix—indicates that matrix inversion can be perfect and thus the image estimation can also be accurate. More generally, if $\kappa(\mathbf{A}) = 10^q$, one may lose roughly q digits of accuracy in the coefficients in the inverse matrix, atop numerical roundoff and other errors. We found $\kappa(\mathbf{A}) = 519$ for the transfer matrix estimated for our system.

3.2. Image computation

Given a transfer matrix $\mathbf{A}$ and measured sensor signals, $\mathbf{y}$, and perhaps some knowledge of properties of the noise $\mathbf{n}$, the task of image computation is to compute an estimate of the target, $\hat{\mathbf{x}}$. We tested several image computation methods. The most traditional approach to such problems is ridge regression or Tikhonov regularization, which yields a multi-dimensional least-squares fit to the data, governed by

$$\hat{\mathbf{x}} = (\mathbf{A}^t\mathbf{A} + \gamma\mathbf{I})^{-1}\mathbf{A}^t\mathbf{y}, \tag{1}$$

where $\mathbf{I}$ is the identity matrix and γ is a scalar regularization parameter that depends upon properties of the noise and source signal. [11] A closely related image computation method is total variation or TV regularization includes a penalty, thereby biasing the estimated image toward images with small total variation. A third method assumes that the sensor signals are a convolution of the source with the spiral point-spread function; then the image can be estimated very efficiently by Fourier methods. [12] If the number of pixels in the photodetector array is n, once the one-time $\mathcal{O}(n^3)$ task of calculating $(\mathbf{A}^t\mathbf{A} + \gamma\mathbf{I})^{-1}$ is complete, then the computational complexity of ridge regression and TV regularization are $\mathcal{O}(n^2)$. Fourier methods are extremely efficient: $\mathcal{O}(n \log n)$. For the current case, the dimensions of $\mathbf{y}$ are 160000 and of $\mathbf{x}$ are 16384; computation of a single image frame by Eq. 1 requires 5.2 *Gflop* and is easily parallelized and implemented in a single FPGA or commodity GPU and executed at video rates.

4. Results

Figure 2 shows two examples of typical still imaging results using ridge regress and TV regularization without post-processing, such as noise filtering. Visual inspection shows these are far superior to those from the earlier PFCA, [3] despite our sensor having 1/37 the area of the PFCA. Videos captured with our sensor appear subjectively higher

in quality than still images because human perceptual effects of temporal coherence and noise rejection. All objects farther than roughly 1 *mm* are in the optical far field of our sensor and hence equally "in focus" and thus the imager's depth-of-field corresponds to roughly 1000 diopters. The overall light sensitivity of an optical imaging system is governed by its f-number, or in our case the numerical aperture ($NA \simeq 0.9$). Our phase gratings pass more than four times the light intensity of stacked amplitude gratings in PFCAs and yield images under normal room illumination.

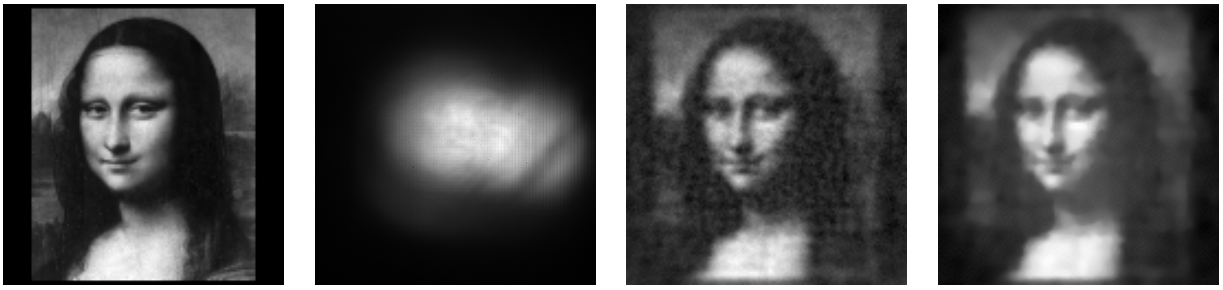

Fig. 2. Left-to-right: Input image as projected onto a screen, raw sensor signals on the photodetector array, final digital image computed by ridge regression and by total variation or TV-norm regression.

5. Conclusions

We have verified experimentally functionality of a new class of diffractive computational imager. Although the imager described above was part of a larger platform, if built alone it would be (to our knowledge) one of the world's smallest image capture devices for its equivalent pixel count, that is, have the lowest physical volume (in mm^3). Such an imager can also be mounted onto existing CMOS chips to add vision capabilities. Finally, the grating and processing can be tailored to a range of application-specific needs including motion estimation, mark reading and image classification.

Acknowledgements

We thank summer interns Avinash Kumar and Patrick Johnstone of the University of the Illinois Urbana-Champaign; Rambus employees Mark Kellam, Evan Erickson, and Thomas Vogelsang for technical assistance, and Michael Ching for strategic support; and David Rowe at Holographix LLC for assistance in grating manufacture and mounting.

References

1. E. R. Dowski, Jr. and W. T. Cathey, "Extended depth of field through wave-front coding," Applied Optics **34**, 1859–1866 (1995).
2. D. G. Stork and M. D. Robinson, "Theoretical foundations of joint design of electro-optical imaging systems," Applied Optics **47**, B64–75 (2008).
3. P. R. Gill, C. Lee, D.-G. Lee, A. Wang, and A. Molnar, "A microscale camera using direct Fourier-domain scene capture," Optics Letters **36**, 2949–2951 (2011).
4. D. G. Stork, "Joint optics/signal processing design for computational diffractive sensing and imaging," in "Computational Optical Sensing and Imaging (COSI)," (Kohala Coast, HI, 2014).
5. P. R. Gill and D. G. Stork, "Lensless ultra miniature imagers using odd-symmetry phase gratings," in "Proceedings of Computational Optical Sensing and Imaging (COSI)," (Alexandria, VA, 2013).
6. P. R. Gill and D. G. Stork, "Digital camera with odd-symmetry spiral phase gratings supports full-resolution computational refocusing," in "Advanced Photonics (Optical Society of America Sensors Congress)," (2013).
7. D. G. Stork and P. R. Gill, "Lensless ultra-miniature computational sensors and imagers," in "SensorComm 2013," (Barcelona, Spain, 2013).
8. P. R. Gill, "Odd-symmetry phase gratings produce optical nulls uniquely insensitive to wavelength and depth," Optics Letters **38**, 2074–2076 (2013).
9. "Aptina MT9J003 spec sheet," (2014). https://www.aptina.com/products/image_sensors/mt9j003i12stcv/.
10. L. Streeter, G. R. Burling-Claridge, M. J. Cree, and R. Künnemeyer, "Optical full Hadamard matrix multiplexing and noise effects," Applied Optics **48**, 2078–2085 (2009).
11. A. Tarantola, *Inverse Problem Theory and Methods for Model Parameter Estimation* (Society for Industrial and Applied Mathematics, Philadelphia, PA, 2005).
12. P. S. R. Diniz, E. A. B. da Silva, and S. L. Netto, *Digital signal processing: System analysis and design* (Cambridge University Press, Cambridge, UK, 2010), 2nd ed.